LANGMUIR

pubs.acs.org/Langmuir Article

Depletion Forces Induced by Mixed Micelles of Nonionic Block Copolymers and Anionic Surfactants

Bhagyashree J. Lele and Robert D. Tilton*

Cite This: *Langmuir* 2020, 36, 10772−10784 Read Online

ACCESS | Metrics & More | Article Recommendations | Supporting Information

ABSTRACT: Depletion forces were measured between a silica sphere and a silica plate in solutions containing nonionic Pluronic P123 poly(ethylene oxide-*b*-propylene oxide-*b*-ethylene oxide) triblock copolymers and anionic sodium dodecyl sulfate (SDS) surfactants using colloidal probe atomic force microscopy. Prior research established synergistic depletion force enhancement in solutions containing SDS and unimeric Pluronic F108 block copolymers via formation of large pseudo-polyelectrolyte complexes. The current work addresses a more complex system where the polymer is above its critical micelle concentration, and surfactant binding alters not only the size and charge of the micelles but also the number of polymers per micelle. Force profiles were measured in 10 000 ppm P123 (1 wt %, corresponding to 1.72 mM based on average molar mass) solutions containing SDS at concentrations up to 64 mM and compared to micellar P123 solutions and to P123-free SDS solutions. Whereas force profiles in the SDS-free micellar P123 solutions were purely repulsive, P123/SDS complexation produced synergistic depletion force enhancement for SDS concentrations between 2 and 32 mM. The synergism that occurred within a finite SDS concentration range was explained by comparing the hydrodynamic size, molar mass, charge, and concentration of depletants in P123/SDS mixtures and their respective single-component solutions obtained with the aid of dynamic light scattering, static light scattering, and dodecyl sulfate ion-selective electrode measurements. These measurements showed that complexation produced effects that would be mutually counteracting with respect to depletion forces: decreasing the mixed micelle hydrodynamic diameter relative to SDS-free P123 micelles would tend to weaken depletion forces, while adding charge and decreasing the aggregation number of polymers per micelle (thereby increasing the number concentration of micellar depletants) would tend to strengthen depletion forces.

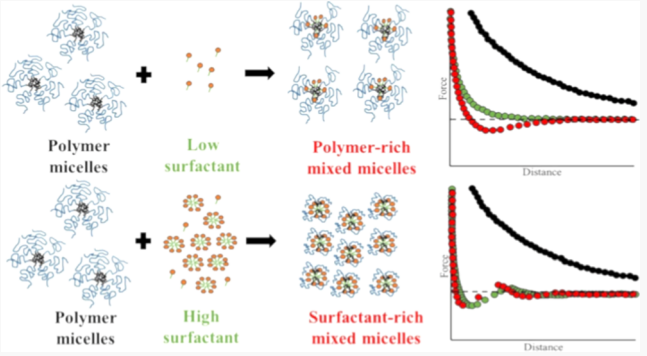

INTRODUCTION

Combinations of nonionic block copolymer amphiphiles and ionic surfactants can be used to tune the performance characteristics of many commercial complex fluid formulations. Since the macroscopic characteristics of a formulated colloidal suspension are engineered by controlling the colloidal forces that act between suspended particles or between particles and bounding surfaces, it is important to develop an understanding of how colloidal forces respond to changes in the composition of multicomponent complex fluid systems that are more representative of practical formulations. Along with the forces described by the DLVO theory,[1] many non-DLVO colloidal forces arise in the presence of macromolecules, including, for example, steric forces,[2,3] bridging forces,[4] and oscillatory structural forces,[5−8] the first attractive minimum of which is known as the depletion force.[9−13] Macromolecules, micelles, nanoparticles, or similar nanoscale objects in solution or co-suspension cause depletion and structural forces between the suspended particles. The depletion force is caused by exclusion of those objects, referred to as "depletants", from the interparticle gap upon sufficiently close approach. Osmotic pressure being a colligative property, the presence of a higher concentration of depletants in the bulk relative to the gap generates an osmotic pressure difference that would drive the particles together, creating an effective attraction force to act in addition to van der Waals attraction.

The original Asakura and Oosawa[9,10] model of the depletion force provides useful insights into how the depletion force may respond to changes in solution conditions. Although the depletion force model has been refined,[14,15] the basic elements of the original model remain valid. The Asakura and Oosawa model maintains that the depletion interaction energy is directly proportional to the depletant osmotic pressure, Π, in the bulk solution. As discussed in detail elsewhere,[16,17] factors

Received: May 27, 2020
Revised: August 2, 2020
Published: August 22, 2020

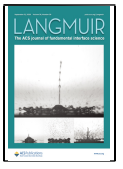

https://dx.doi.org/10.1021/acs.langmuir.0c01574
Langmuir 2020, 36, 10772−10784

such as an increased depletant concentration, size, or charge that would increase the depletant osmotic pressure tend to strengthen the depletion attraction. Charged polyelectrolytes tend to yield stronger depletion interactions than similarly sized, uncharged depletants at similar concentrations, due to the counterion osmotic pressure[11,18−20] and to the occurrence of an electrostatic exclusion zone that enhances the depletion layer thickness. These trends are well established by measurements and theoretical predictions for solutions or suspensions containing a single type of depletant, including spherical[21,22] or nonspherical[23] nanoparticles, nonionic polymers,[24−27] polyelectrolytes,[18,28] and ionic surfactant micelles.[29,30]

Depletion forces in multicomponent systems are seldom investigated, but there have been a few prior studies for solutions of mutually attractive depletants.[17,31−33] Tulpar and co-workers[31] first observed synergistic enhancement of the depletion force between a silica sphere and a flat silica plate caused by the charged supramolecular assemblies that form by complexation of Pluronic F108 poly(ethylene oxide-*b*-propylene oxide-*b*-ethylene oxide) nonionic triblock copolymers with anionic sodium dodecyl sulfate surfactants (SDS). Further examination of that system showed that synergistic enhancement of both depletion attraction and the first repulsive barrier of the oscillatory structural force was confined to a finite range of surfactant-to-polymer concentration ratios, which depended on the electrolyte concentration.[17] Complexation of the anionic surfactants with the nonionic polymers generated pseudo-polyelectrolyte complexes, which were negatively charged by virtue of the bound surfactants and which were larger than either uncomplexed polymers or surfactant micelles. Just as counterions increase the osmotic pressure of a polyelectrolyte in solution, the osmotic pressure enhancement from counterions to the pseudo-polyelectrolyte complexes was a major cause of the observed synergism. In the F108/SDS system, depletion force synergism occurred at a fixed total concentration of depletants.[17]

Depletion and oscillatory force synergism has also been observed in a mixture of two mutually repelling depletants, sodium polyacrylate (Na-PAA) and SDS, that have no tendency to form complexes with each other.[16] Mixing two such charged components enhanced depletion forces primarily by synergistically increasing the depletant concentrations. Ionic screening from PAA counterions decreased the critical micelle concentration (CMC) of SDS, and screening via SDS weakened the dipole−dipole interactions that drive polyelectrolyte clustering in solution. The production of more SDS micelles and the liberation of individual PAA chains from clusters so they could then act as independent depletants produced the depletion force synergism.

Prior work has focused on depletion forces in mixtures of surfactants and nonmicellar polymers. In this work, we now determine how depletion forces may be altered when surfactants bind to a polymer amphiphile when the polymer is well above its normal critical micelle concentration (CMC), using anionic SDS and Pluronic P123 PEO−PPO−PEO triblock copolymers as a model system. Supramolecular assemblies formed by polymer/surfactant complexation in solution have been thoroughly studied and reviewed.[34−44] Complexation of Pluronic micelles with SDS proceeds via a progression of Pluronic micelle disintegration, whereby the larger polymer micelles experience three different binding regimes as a function of increasing SDS concentration: polymer-rich mixed micelles, succeeded by a bimodal distribution of polymer-rich and SDS-rich mixed micelles, and finally SDS-rich mixed micelles.[44−48] This was originally described as a "peel-off" process to convey the idea that the mixed micelles contain fewer polymer chains than the surfactant-free polymer micelles do.[44] Pluronic P123 has a significantly lower CMC (and lower critical micelle temperature for a given concentration) than the F108 copolymer that was previously investigated for depletion force synergism, and it has been shown to exhibit this three-regime micellar interaction with SDS.[44,45]

With a rich variety of compositions, sizes, and charges of polymer/surfactant complexes that can form as a function of the SDS/P123 ratio, one may anticipate a more complicated depletion force landscape in mixtures when the Pluronic concentration exceeds its normal CMC, compared to the nonmicellar F108 system. Colloidal probe atomic force microscopy (CP-AFM) was used in this study to measure the net force profile between a negatively charged silica sphere and silica plate in the presence of aqueous solutions containing a fixed concentration of Pluronic P123 well above its CMC and varying concentrations of SDS. Complexation synergistically enhanced depletion forces at low SDS concentrations but not at high SDS concentrations.

To better understand these trends in depletion forces, a detailed characterization of the P123/SDS complexes was performed. Dynamic light scattering, static light scattering, and dodecyl sulfate ion-selective electrode measurements were used to investigate the size, composition, charging, and concentration of the depletants that generated the observed depletion forces. The current work extended the prior characterization of P123/SDS complexes by performing Zimm plot static light scattering analysis at low SDS concentrations to find the molar mass and second virial coefficient of the complexes. Combining Zimm plot analysis with dodecyl sulfate ion-selective electrode measurements revealed the average number of SDS molecules bound per P123/SDS complex. That information complemented dynamic light scattering analysis of the concentration dependence of the hydrodynamic size of the complexes and the conditions under which P123/SDS mixtures contain monomodal or bimodal distributions of the complexes. Separate ellipsometry measurements were performed to check for a possible effect of P123 and/or SDS adsorption to silica on the net interaction force. Overall, this study showed that the finite SDS concentration range for synergistic depletion force enhancement was dictated by an interplay of competing factors, some favoring and others suppressing depletion forces. The manner in which this mechanism contrasts with the F108/SDS system will be discussed.

EXPERIMENTAL SECTION

Materials. Pluronic P123, a nonionic triblock copolymer with the composition PEO_{20}−PPO_{70}−PEO_{20} (molar mass 5800 g/mole), was provided by BASF Corp. Sodium dodecyl sulfate (SDS) was purchased from Sigma-Aldrich (BioXtra grade, >99% purity) and was used as received. Purity was confirmed by the absence of a minimum in the surface tension isotherm near the CMC. All samples contained 0.1 mM NaCl (Biotechnology grade, VWR Life Science) as the background electrolyte, and samples containing SDS were freshly prepared on the day of each experiment. Water for all experiments was purified to 18.2 MΩ cm resistivity using a ThermoFisher Barnstead Nanopure Diamond system. For dodecyl sulfate surfactant-selective electrode measurements, Orion 810007 and Orion 900002 electrode filling solutions (ThermoFisher Scientific) were used as

https://dx.doi.org/10.1021/acs.langmuir.0c01574
Langmuir 2020, 36, 10772−10784

inner and outer chamber filling solution for the Orion 900200 Sure-Flow Reference Half-Cell Ag/AgCl double junction electrodes. KCl for electrode measurements was purchased from Fisher Biotech (Enzyme grade). The cationic surfactant used to make the dodecyl sulfate-selective membrane, cetyltrimethylammonium bromide (CTAB), was purchased from Sigma-Aldrich (BioXtra grade, >99% purity).

METHODS

Colloidal Probe Atomic Force Microscopy. All forces were measured between a spherical silica particle and a flat silica plate using the CP-AFM technique[49] with a Bruker Multimode VIII AFM, operating in contact mode. Colloidal probe fabrication and characterization, AFM fluid cell assembly, and substrate cleaning were conducted as described previously.[16,17] Colloidal probes with a nominal diameter of 10 μm (Corpuscular Inc.) were affixed to tipless cantilevers having a nominal 0.02 N/m spring constant (Bruker MLCT-O10, B). Spring constants were measured using the thermal tuning method.[50] Flat fused silica discs with a diameter of 12.7 mm, thickness of 3.18 mm, and RMS roughness of 0.5 nm were purchased from CVI Laser Optics. Cleanliness was verified prior to each CP-AFM experiment by measuring the highly reproducible electrostatic double-layer repulsion between the bare silica probe and the bare disc in 0.1 mM NaCl solution, including the lack of adhesion between surfaces in contact as attributed to hydration forces.

After filling the fluid cell by pumping 10 cell volumes of sample solution through the cell, the system was allowed to equilibrate under quiescent conditions for 15 min before measuring forces. The sphere-to-plate approach and retract speeds were kept below 60 nm/s to decrease the hydrodynamic force on the cantilever to the point where it did not influence measured force curves.[16,17,51] For each solution composition, force curves were recorded at five different locations on the disc surface and an average force curve was calculated. This procedure was repeated in at least three independent experiments with freshly prepared solutions, discs, and colloidal probes. All experiments were conducted in the temperature range of 22 ± 2 °C. All forces were normalized by the colloidal probe radius that was measured by scanning electron microscopy (Hitachi 2460-N).

Ellipsometry. Ellipsometry measurements were performed to obtain the surface excess concentration of P123/SDS complexes on silica surfaces in aqueous solutions using a phase-modulated ellipsometer (Beaglehole Instruments Picometer) with a polarized 632.8 nm laser beam.[52] Silicon wafers with a 2.3 nm thick native oxide layer were used for the adsorption measurements, following previously described procedures.[53,54] All samples contained 10 000 ppm P123 (1 wt %, corresponding to 1.72 mM based on the average molar mass) and 0.1 mM NaCl. The substrate was sequentially exposed to a series of solutions containing different SDS concentrations at 22 ± 2 °C, in the order of decreasing concentration. Once the ellipsometric signal had stabilized after each change of solution composition, the Δx and Δy ellipsometric parameters defined by Beaglehole[52] were analyzed as a function of the incident angle to obtain the optical average thickness of the adsorbed P123/SDS layer. TF Companion software (Version 3.0, Semicon Software Inc.) was used to determine the optical average adsorbed layer thickness for an assumed refractive index of 1.465 for the P123/SDS layers. The total surface excess concentrations of the P123/SDS adsorbed layers were calculated via the de Feijter equation[55,56] from the thickness and the assumed refractive index values, using a refractive index increment of 0.138 cm^3/g measured for SDS by differential refractometry (AR7 Automatic Digital Refractometer, Reichert Technologies Analytical Instruments). Since Pluronics and SDS have similar refractive index increments, this value was used to represent the complexes.[57] As discussed elsewhere,[55−57] the value of the assumed refractive index of the adsorbed layer does not affect the calculated surface excess concentration for the adsorbed layers, since errors in index and thickness are mutually compensating.

Dodecyl Sulfate Ion-Selective Electrode Analysis. The dodecyl sulfate (DS^-) ion-selective electrode was fabricated using two commercially available Orion 900200 Sure-Flow Reference Half-Cell Ag/AgCl double junction electrodes and implemented with an Orion Star A329 potentiometer, as described in Supporting Information, Section I. Selectivity for DS^- ion was based on a membrane prepared by adapting the procedure suggested by Wang and co-workers.[58] The electrode setup was used to obtain the concentration of free, uncomplexed DS^- in solutions containing 10 000 ppm P123. All electrode measurements were conducted at 22 ± 2 °C. The electrode was calibrated against a series of polymer-free SDS solutions. The inner filling solution was replaced for each sample to ensure reproducibility. The DS^- ion activity for the P123/SDS mixtures was first measured at the highest SDS concentration, and then, the sample was diluted using the constant-concentration polymer solution to produce lower SDS concentrations. After each dilution, the solution was gently stirred with a magnetic stir bar for 2 min and the electromotive force (EMF) was noted. It was converted to activity of free DS^- ions using the electrode constants obtained from the calibration with SDS solutions[59] below the CMC, whereby all SDS existed as a fully dissociated 1:1 electrolyte. The analysis used to determine the concentrations of free and polymer-bound DS^- based on the Debye−Hückel activity coefficient model[60] is developed in the Results and Discussion section.

Static Light Scattering. The molar mass and second virial coefficient of the P123/SDS complexes formed with varying SDS concentrations were determined by Zimm plot analysis of static light scattering data obtained using a BI-200 SM Brookhaven goniometer. All samples were filtered for static light scattering using 0.2 μm polyethersulfone syringe filters. Static light scattering measurements were conducted at 23 °C. Special considerations for data collection and Zimm analysis are noted in the Results and Discussion section.

Dynamic Light Scattering. Hydrodynamic diameters of the P123/SDS complexes formed in the presence of varying SDS concentrations were measured by dynamic light scattering using a Malvern Zetasizer Nano ZS at the 173° backscatter angle. All samples were filtered for dynamic light scattering using 0.2 μm polyethersulfone syringe filters. These measurements were conducted at 23 °C. Autocorrelation functions were fitted using the non-negative least squares (NNLS) method to determine intensity-weighted distributions of the translational diffusion coefficients for 10 000 ppm P123 samples with varying SDS concentrations. The corresponding hydrodynamic diameters of the complexes were calculated via the Stokes−Einstein equation.

RESULTS AND DISCUSSION

We have studied the impact of complexation between micellar P123 and SDS at varying concentrations on the interaction forces between negatively charged silica spheres and fused silica discs. In the following sections, the interaction forces are presented first, followed by a detailed characterization of P123/SDS complexes that aid in the interpretation of the interaction force trends. To help put the force profile interpretations in the section below into context, the key features of P123/SDS complexation are briefly highlighted in advance here: Characterization results confirmed the three-regime disintegration of large, uncharged P123 micelles into two types of charged species with different sizes—large P123-rich mixed micelles and small SDS-rich mixed micelles. Complexation with P123 occurred at SDS concentrations as low as 0.001 mM, and the complexation had not yet saturated at 64 mM, the highest SDS concentration considered in the force measurements. The micelle molar mass decreased by ∼85% relative to surfactant-free P123 micelles for an SDS concentration of 1.25 mM. The mixed micelle distribution was monomodal for these small SDS concentrations. The SDS concentration of 1.25 mM also marked the point at which the mixed micelles contained approximately equal numbers of polymer chains and surfactants. Further increasing the SDS

https://dx.doi.org/10.1021/acs.langmuir.0c01574
Langmuir 2020, 36, 10772−10784

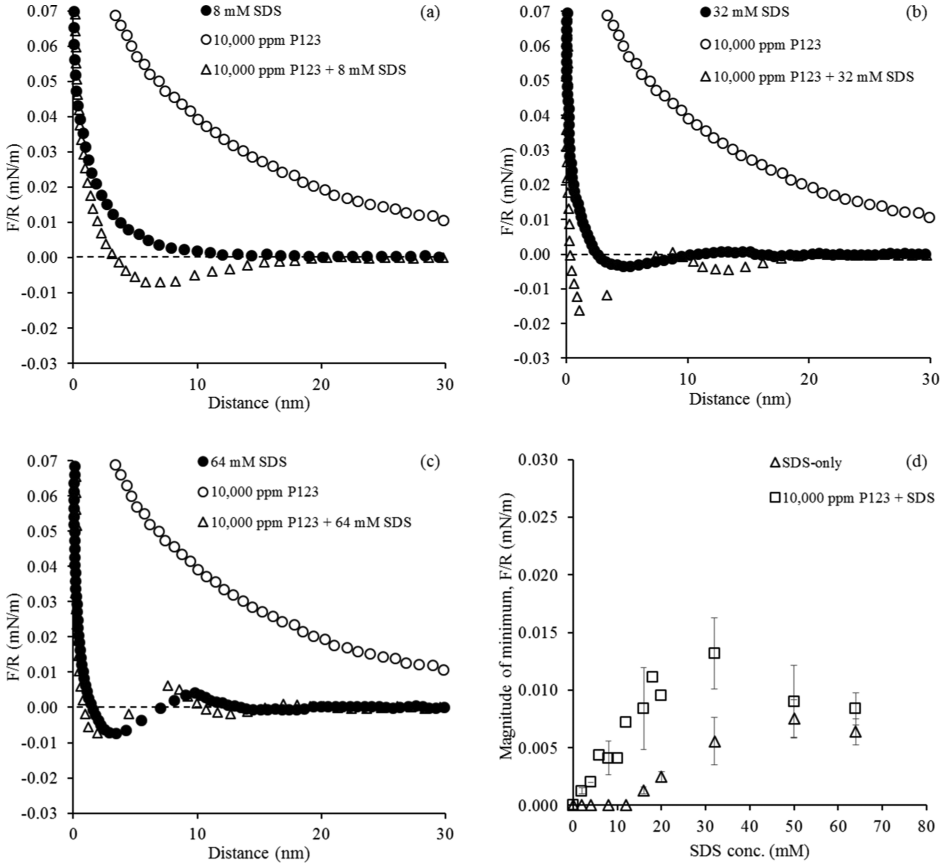

Figure 1. Representative normalized force profiles for selected SDS concentrations with 10 000 ppm P123: (a) 8 mM SDS, (b) 32 mM SDS, and (c) 64 mM SDS. The purely repulsive force profile for the single-component 10 000 ppm solution of P123 is repeated in panels (a)−(c) for comparison. (d) Summary of the magnitude of the primary minimum in net force profiles for various SDS concentrations, with and without 10 000 ppm P123. Error bars in (d) are standard error of the mean from three replicates. All samples contained 0.1 mM NaCl.

concentration produced bimodal micelle distributions that shifted in favor of the SDS-rich mixed micelles with increasing SDS concentration. The mixed micelles formed at the highest concentrations considered had a size and an average number of surfactants bound per polymer chain that closely resembled the size and aggregation number of normal SDS micelles. The main outcome of these effects is a progressive increase of both the concentration and the charge of the mixed micelles that serve as depletants, albeit with complex shifts in the mixed micelle size distributions.

Force Curve Analysis. Complexation between P123 and SDS produces anionic mixed micelles[44,45] with a charge and size that vary with the binding extent. Figure 1 shows that these mixed micelles generate significantly different interaction force profiles as compared to their respective single-component solutions. The normalized force profiles were measured in solutions containing 10 000 ppm P123, which was well above the 500 ppm (0.086 mM) CMC that has been reported for P123 at 22.5 °C.[61] The SDS concentration was varied from 0 to 64 mM, spanning from below to well above the SDS CMC of ∼8 mM. Panels (a) through (c) directly compare representative force profiles for a mixture and a polymer-free SDS solution at a selected SDS concentration as well as a force profile for SDS-free P123 solution. Force profiles for 10 000 ppm P123 with the remaining set of SDS concentrations examined are presented in Supporting Information, Section II. When interpreting CP-AFM force measurements, note that the zero of separation distance corresponds to the onset of the regime of constant cantilever compliance and may not always indicate direct contact between the bare silica surfaces.

Despite the presence of P123 micelles, the force profile was purely repulsive in SDS-free solutions of 10 000 ppm P123. The distance range presented in Figure 1 was truncated to highlight differences among the mixtures. The repulsive force for the P123 solutions of course decayed smoothly to zero at larger distances. The lack of an attractive minimum does not necessarily mean that there was no depletion force. The decay length of the long-range force was 15.5 nm. This was smaller than the Debye length for the electrostatic double-layer repulsion at 0.1 mM NaCl (30.3 nm), indicating that the net force was not just the electrostatic double-layer repulsion. The forces for P123 by itself may be consistent with the presence of a moderate depletion attraction superimposed on the double-layer repulsion. This depletion attraction would have to be weaker than the double-layer repulsion at all separation distances measured. The possibility that the net force was influenced by a steric repulsion between the adsorbed P123 layers is addressed below, but first the possibility is considered that P123 adsorption may have altered the contribution of electrostatic double-layer forces to the net force.

In contrast to P123, forces measured between silica surfaces in the absence of SDS in 0.1 mM NaCl solutions containing nonmicellar Pluronic F108, at either 1000 or 10 000 ppm, were indistinguishable from the measured electrostatic double-layer repulsion, both in magnitude and decay length.[17] F108 did adsorb to silica in the absence of SDS, but the force profile data

https://dx.doi.org/10.1021/acs.langmuir.0c01574
Langmuir 2020, 36, 10772−10784

showed that adsorption did not change the silica surface charge density to a significant extent. Although it did not occur with F108, it remains possible that P123 adsorption could have decreased the surface charge density, for example, if it sufficiently decreased the dielectric constant close to the silica surface. This would decrease the magnitude of the double-layer repulsion, but it would not decrease the Debye length. The degree to which such a suppression of the double-layer repulsion may have influenced the forces measured with P123 by itself is not yet known, but it cannot be the sole cause of the effect of P123 on the force profile, since the measured decay length was significantly smaller than the Debye length. The possibility that the net force was influenced by a steric repulsion between the adsorbed P123 layers is addressed next.

Ellipsometry measurements showed that there was adsorption from 10 000 ppm P123 solutions to negatively charged silica surfaces at SDS concentrations of 7.5 mM and below in the presence of 0.1 mM NaCl (Figure 2). Adsorption did not occur for mixtures at higher SDS concentrations, due to the increasing negative charge on the P123/SDS complexes and their associated electrostatic repulsion from the negatively charged silica surface. This was consistent with the prior results for Pluronic F108 co-adsorption with SDS.[57] Thus, at low SDS concentrations (but not at any SDS concentration exceeding 7.5 mM), electrosteric repulsions (or steric in the absence of SDS) may have contributed to the net force measurement. The short-range steric force was not probed in these measurements that use low spring constant cantilevers.

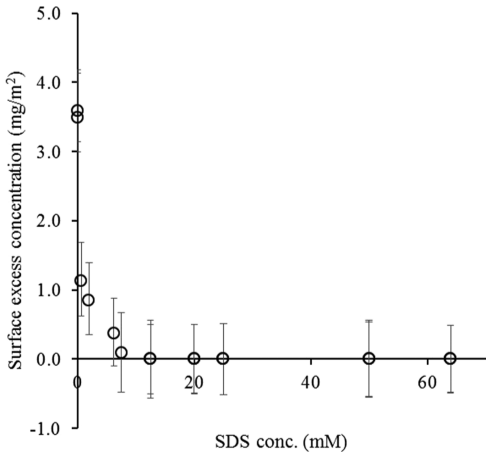

Figure 2. Surface excess concentration of P123/SDS complexes adsorbed on silica as a function of SDS concentration. All samples contained 0.1 mM NaCl and 10 000 ppm P123. Error bars are based on the uncertainty of ellipsometric parameter fitting.

In the absence of P123, 8.0 mM SDS (Figure 1a) yielded a purely repulsive force profile with a 3.5 nm decay length, consistent with the 3.4 nm Debye length calculated for the ionic strength of this solution. This was just below the CMC, and as expected, SDS acted as a fully dissociated 1:1 electrolyte.[29−31] In contrast, the force profile in the mixture of 10 000 ppm P123 and 8.0 mM SDS contained an attractive primary minimum, confirming a synergistic depletion force enhancement in P123/SDS mixtures with 8.0 mM SDS.

Increasing the SDS concentration beyond the CMC to 32 mM (Figure 1b) in the absence of P123 produced an attractive well of approximately 0.004 mN/m at ∼5.3 nm separation distance due to depletion attraction caused by SDS micelles. The mixture of 32 mM SDS and 10 000 ppm P123 produced a primary attractive minimum that was significantly deeper than the P123-free SDS solution and was shifted to smaller separation distances. Whereas the SDS-free P123 solution yielded a purely repulsive interaction profile, synergistic depletion force enhancement occurred in the mixture with 32 mM SDS. The inward shift of the attractive minimum in the mixture relative to that in the polymer-free SDS solution is meaningful. There was no adsorption to silica under these conditions, so the apparent zero separation distance likely corresponded to bare silica contact. The inward shift was thus consistent with a strengthened depletion attraction superimposed on the partially screened electrostatic repulsion between the surfaces. The subtleties of the interplay between polymer/surfactant complexation and the relative extent of double-layer screening were discussed in more detail previously.[17]

Notably, although there were two distinct force minima, the local maximum between them was reproducibly a small negative force (attractive), as opposed to the well-formed repulsive force barrier that is expected for monodisperse depletants. The deepening of the force minimum is consistent with an increased concentration of the depletants. The general shift in the overall force profile to more attractive forces without a repulsive barrier separating local minima is reminiscent of a similar shift in the PAA/SDS system where mutually repelling anionic surfactant and anionic polyelectrolyte depletants co-exist in solution.[16] Dynamic light scattering (presented below) has confirmed that at 32 mM SDS, there were two distinct peaks in the hydrodynamic diameter distribution. This indicates that two distinct types of co-existing depletants could separately contribute to depletion forces at different separation distances for these conditions, as occurred in the PAA/SDS system.

Further increasing the SDS concentration to 64 mM (Figure 1c) eliminated the synergistic depletion force enhancement. Force profiles in the mixture were similar to those measured in the polymer-free SDS solution. Figure 1d summarizes how the depth of the primary minimum in the net force profile depended on the SDS concentration in the presence or absence of P123. In the absence of the polymer, a depletion attraction minimum was detected only at and above 16 mM SDS. In the presence of 10 000 ppm P123, a depletion minimum was observed for SDS concentrations as low as 2 mM. This synergistic enhancement of depletion forces strengthened with increasing SDS concentration, up to a maximum enhancement at 32 mM SDS.

Beyond 32 mM SDS, the enhancement weakened. Force profiles for the mixture and the polymer-free SDS solutions were similar to each other at both 50 and 64 mM SDS. The force minima measured for mixtures with these SDS concentrations were within experimental error of those measured in polymer-free SDS solutions. Since increasing SDS concentration increases the extent of binding to the polymer up to some saturation point, it is clear that more extensive complexation must have contributed to the synergistic depletion force enhancement with increasing SDS concentration. While the increasing charge of the complexes, and the corresponding counterion enhancement of the osmotic pressure, would promote depletion force enhancement, other factors may be important as well. For example, SDS/P123 binding could change the micellar aggregation number and thereby change the total concentration of the depletants as the

https://dx.doi.org/10.1021/acs.langmuir.0c01574
Langmuir 2020, 36, 10772−10784

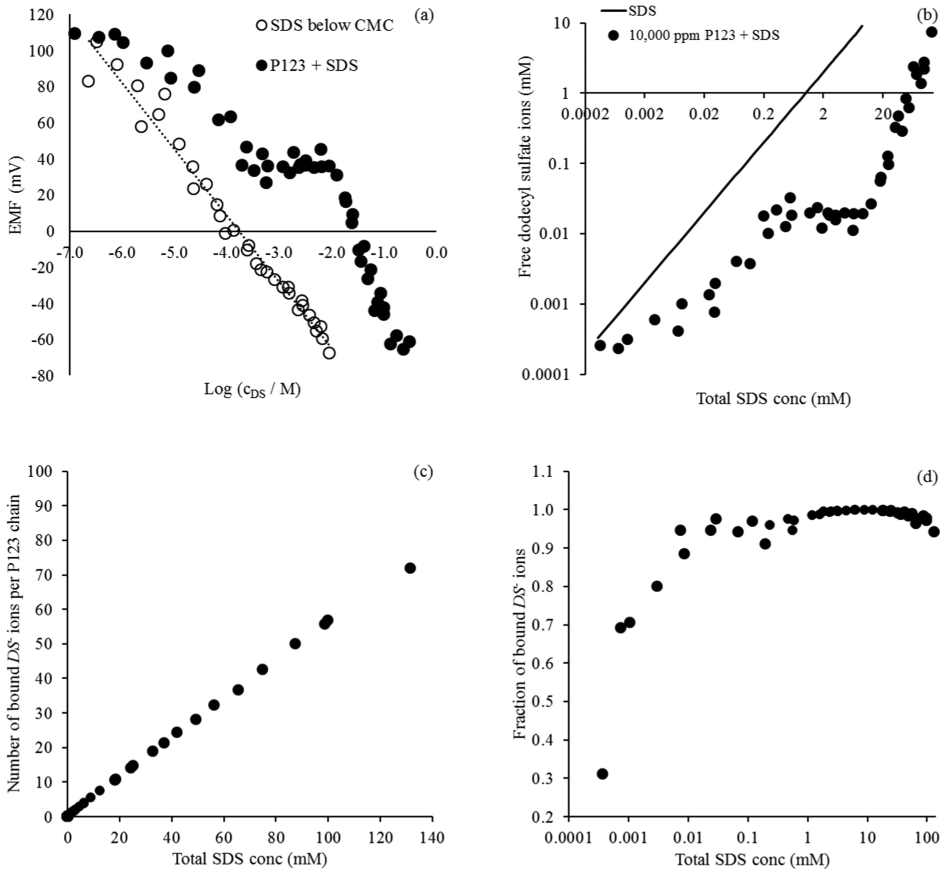

Figure 3. (a) EMF measured as a function of the total SDS molar concentration in the absence or presence of 10 000 ppm P123. (b) Calculated free dodecyl sulfate ion concentration from EMF measurements in the presence of 10 000 ppm P123, with the polymer-free SDS 1:1 line for reference. (c) Average number of bound DS^- ions per P123 chain as a function of total SDS concentration. (d) Fraction of added DS^- bound to the polymer as a function of total SDS concentration. All samples contained 0.1 mM NaCl.

SDS concentration is increased for a fixed P123 concentration. To better understand not only the strength of the depletion force synergism but also its occurrence over a finite concentration range, the sections below present the characteristics, concentrations, and types of the depletants formed by complexation as a function of SDS concentration.

Characterization of P123/SDS Mixed Micellar Complexes. *Dodecyl Sulfate Ion-Selective Electrode Analysis.* Self-assembly of SDS, whether in the form of free micelles or polymer-bound complexes, limits the activity of DS^- ions in solution. When solutions are analyzed with a DS^--selective electrode based on a selective membrane, the presence of DS^- ions produces a membrane potential that depends on the free DS^- concentration. In the apparatus used here, the reference electrodes were at a constant potential, and the change in the measured electromotive force (EMF) was dependent only on the change in membrane potential.

Figure 3a shows the measured EMF as a function of the total SDS concentration in the absence or presence of 10 000 ppm P123. The polymer-free data was used as the calibration for assays of the free DS^- concentration in the presence of P123. Data is plotted in Figure 3a only up to the CMC; beyond that point, the EMF depended on concentration in a nonlinear manner and was not needed for the assay of SDS/P123 mixtures. The DS^- activity was calculated from the SDS concentration using the Debye–Hückel limiting law for the molal activity coefficient γ_{DS}[60,62]

$$\log_{10}(\gamma_{DS}) = -Az_{DS}^2\sqrt{I} \quad (1)$$

where I is the ionic strength of the sample, z_{DS} is the valence of dodecyl sulfate ions (-1), and A is a constant equal to 0.514 $mol^{-1/2}$ $kg^{1/2}$ for aqueous solutions at 23 °C. The measured EMF for 10 000 ppm P123 solutions at varying concentrations of SDS is also plotted in Figure 3a. The EMF in the presence of the polymer deviates from the EMF measured in SDS-only solutions at SDS concentrations greater than approximately 0.001 mM.

When assaying free DS^- in solution in the presence of P123, the measured activity was converted back to free DS^- concentration using the Debye–Hückel activity coefficient, and the plot of free DS^- concentration vs total SDS concentration in the presence of 10 000 ppm P123 was generated (Figure 3b). The contribution of SDS to the ionic strength values used in activity coefficient calculations was assumed to be solely due to dissociated sodium counterions. This decision was based on the analysis of ionic strength in ionic micellar solutions.[63] As the degree of sodium ion dissociation from the P123/SDS complexes was unknown, it was assumed to be the same as for SDS micelles, 23%.[17,64,65] This was previously shown to be valid for F108/SDS complexes.[17] Since the onset of SDS binding to P123 occurred at extremely low concentrations, and the free DS^- concentration was consistently small relative to the total SDS concentration (Figure 3b), the ionic strength contribution from free DS^- was neglected. The quantitative consequences

https://dx.doi.org/10.1021/acs.langmuir.0c01574
Langmuir 2020, 36, 10772–10784

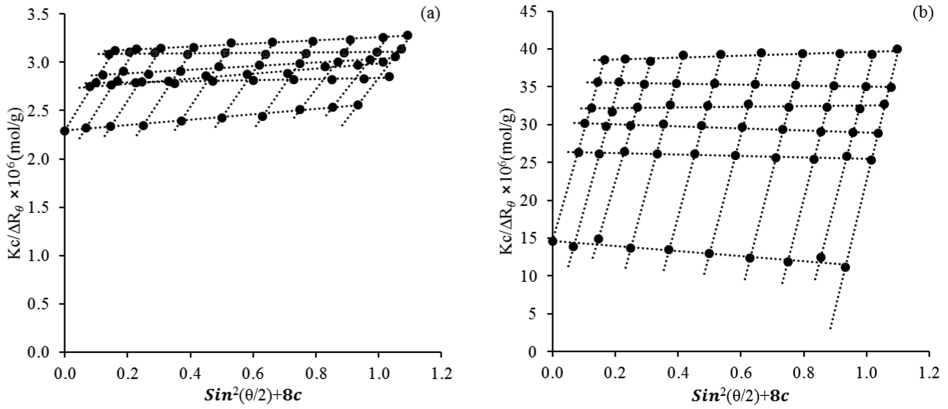

Figure 4. Zimm plot analyses for (a) SDS-free P123 solutions (SDS/P123 mass ratio = 0) and (b) SDS/P123 mass ratio = 0.035. All samples contained 0.1 mM NaCl.

of this assumption were modest. Had an extreme 100% degree of dissociation been assumed, it would have caused a deviation of less than 10% at the SDS concentrations considered in the force curve measurements.

Three different P123/SDS binding regimes were identified based on the slopes in Figure 3b. A region of constant slope of increasing free DS^- concentration from 0.001 to 0.2 mM total SDS concentration transitioned to a region of constant free DS^- concentration (of 0.02 mM) up to a total concentration of 10 mM, followed by another region of constant slope of increasing free DS^- concentration up to a total SDS concentration of 131 mM. The free DS^- concentration was below the CMC of SDS at all total SDS concentrations up to 131 mM. This confirmed that there were no free SDS micelles in the presence of P123 in any of the CP-AFM force measurements.

The observation that the total SDS concentration could exceed the CMC by a factor of ∼15 without producing free micelles in solution in the presence of 10 000 ppm P123 indicates that polymer/surfactant binding continued throughout the concentration range of the CP-AFM experiments. Binding continued well beyond the 10 mM total SDS concentration that marked the end of the zero slope regime in Figure 3b. The significant discrepancy between the free and total DS^- concentrations at low SDS concentrations confirmed that the critical association concentration (CAC) for SDS binding to P123 was very low, approaching 0.001 mM SDS. Finally, the region of constant free DS^- concentration between 0.2 and 10 mM total SDS concentrations indicates a cooperative, micellization-like binding in that concentration range.

The binding isotherm for the average number of DS^- ions bound per P123 chain calculated from the data in Figure 3b is plotted in Figure 3c. This binding isotherm is averaged over all polymer chains, without regard to changes in the micellization state of the polymer chains themselves. Consistent with the discussion above, binding commenced at extremely low SDS concentrations, but it had not yet saturated at SDS concentrations as large as 131 mM. The average number of DS^- bound per P123 chain increased linearly to approximately 70 at 131 mM SDS, which was very close to the aggregation number reported elsewhere for free SDS micelles.[64,65] Beyond 131 mM, the free DS^- concentration had reached the normal SDS CMC, suggesting that no further polymer binding would occur. The fraction of the total amount of added DS^- ions that were bound to P123 is plotted in Figure 3d. The fraction rapidly increased to nearly unity for SDS concentrations above ∼0.01 mM. For the entire range of SDS concentrations considered in the CP-AFM force measurements, nearly 100% of the added SDS was bound to P123.

The implications of these results for interpreting force measurements are as follows: As the number of bound DS^- ions per P123/SDS complex increased, the charge per complex would increase monotonically. This is because the degree of sodium counterion binding to P123-bound DS^- must be less than unity. A nearly constant ∼23% degree of counterion dissociation from Pluronic F108-bound DS^- was reported previously.[17] Thus, increasing SDS concentration would increase the net negative charge of the complexes that act as depletants. The similarity of the number of DS^- bound per P123 chain at high SDS concentrations and the previously reported aggregation number of free SDS micelles suggests that the P123/SDS complexes formed at high SDS concentrations closely resemble free SDS micelles. The resemblance of the primary depletants in P123 mixtures with high SDS concentrations to free SDS micelles is consistent with the loss of depletion force synergism that occurred at the highest SDS concentration (see Figure 1c,d). Additional insight into the nature of the primary depletants in different SDS concentration ranges is obtained from light scattering measurements reported below.

Static Light Scattering. The osmotic pressure difference that drives the depletion attraction increases as the number concentration and charge of the depletants increase. The concentration of the depletants, whether they are SDS micelles or P123/SDS mixed micelles, can be calculated from the known total mass concentration provided the molar mass of the depletant is known. In the case of P123/SDS mixed micelles, where ∼100% of DS^- is bound to the polymers, one only requires the total concentration of P123 and SDS at a particular SDS/P123 mass ratio and the molar mass of the mixed micelles that form at that ratio. The latter was determined by Zimm plot analysis of static light scattering data.

The analysis was performed at four different SDS/P123 mass ratios: 0, 0.0023, 0.011, and 0.035, ensuring that a single type of P123/SDS mixed micelle was present for a particular mass ratio. It was confirmed using dynamic light scattering for 10 000 ppm P123 (see the section below) that the P123/SDS complexes that formed in this range of mass ratios had

https://dx.doi.org/10.1021/acs.langmuir.0c01574
Langmuir 2020, 36, 10772−10784

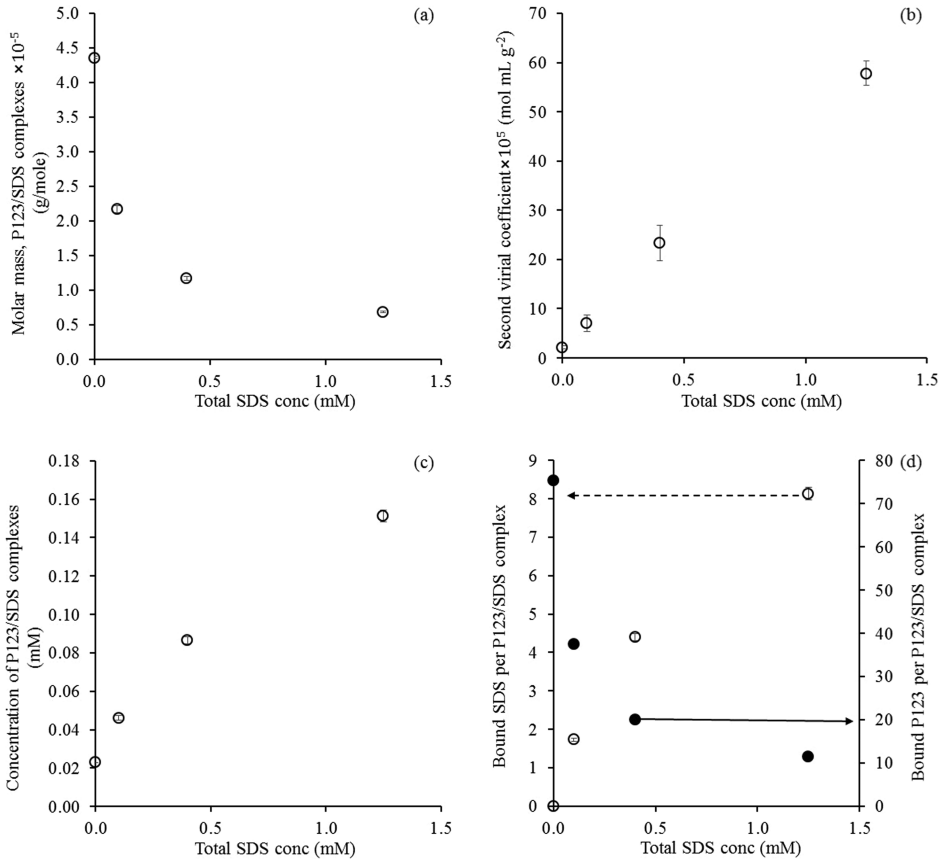

Figure 5. (a) Molar mass of the P123/SDS mixed micelles as a function of total SDS concentration. (b) Second virial coefficient of the P123/SDS mixed micelles as a function of total SDS concentration. (c) Concentration of the P123/SDS mixed micelles as a function of total SDS concentration. (d) Numbers of bound SDS and bound P123 molecules per P123/SDS mixed micelle as a function of total SDS added. Error bars in molar mass (smaller than the symbols in panel a) and second virial coefficient are uncertainties from fitting Zimm plots. Calculated quantities correspond to 10 000 ppm P123.

monomodal size distributions. The results are provided for SDS-free P123 solutions and for SDS/P123 = 0.035 in Figure 4. It was assumed that at each ratio, the properties of the P123/SDS complexes remained unchanged as the total concentration was changed, since the SDS concentration was above the CAC, ∼100% of the added DS^- was bound to the polymers, and the complexes were not saturated. Increasing the total SDS and P123 concentration at a fixed ratio simply increased the concentration of the P123/SDS complexes. This assumption that the surfactant/polymer ratio fixes the properties of the complexes has been invoked successfully for SDS complexes with poly(ethylene oxide) homopolymers[66] and for nonmicellar Pluronic F108.[17] Details of the Zimm analysis that support the validity of this assumption will be noted below, along with further support to come from dynamic light scattering.

The concentration of P123 was maintained above its CMC (500 ppm) for all of the mass ratios. For each ratio, the samples were tested with five different P123 concentrations, 10 000, 12 500, 15 000, 17 500, and 20 000 ppm, and scattering intensities were recorded at nine different scattering angles from 30 to 150°. Zimm plots for all of the P123/SDS complexes had negative slopes for the reciprocal scattering intensity vs scattering angle plots in the limit of zero concentration, as has been observed previously for ionomer solutions where scattering was strongly influenced by electrostatic interactions.[67] In this case, it is not possible to determine the radius of gyration of the scatterers without making additional assumptions. Thus, although R_G was not determined, this characteristic negative slope confirmed the strong charging of the complexes. At all of the ratios studied, the Zimm plots had straight line fits across the full concentration range. This supports the assumption that the properties of the complexes did not change as the total concentration changed at a fixed SDS/P123 mass ratio. Note that the static light scattering analysis was restricted to low SDS concentrations (consistently less than 2 mM) where complexation produced a single type of P123/SDS species. Dynamic light scattering results (to be shown below) revealed the formation of bimodal complexes at higher SDS concentrations.

While the dominant influence of electrostatic interactions precluded the calculation of R_G for the complexes, the Zimm analysis did yield the molar mass and second virial coefficient for the complexes formed at different SDS/P123 ratios. These are plotted as a function of SDS concentration in Figure 5a,b. The Zimm analysis was performed separately for each of the fixed SDS/P123 mass ratios. This yielded the molar mass and second virial coefficient of the complexes that formed at that particular ratio. To interpret the CP-AFM data, it is necessary to show how these properties change with a change in surfactant concentration for a 10 000 ppm P123 solution. Thus, each calculated point in Figure 5 corresponds to a 10 000 ppm P123 solution analyzed separately for each of four different SDS/P123 ratios and then plotted according to the

https://dx.doi.org/10.1021/acs.langmuir.0c01574
Langmuir 2020, 36, 10772−10784

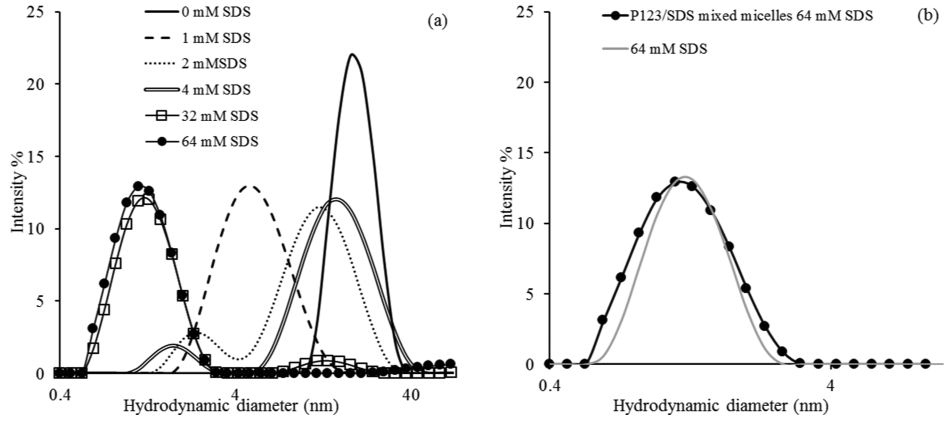

Figure 6. (a) Intensity-weighted hydrodynamic diameter distributions for P123/SDS complexes with 10 000 ppm P123 and various SDS concentrations. (b) Hydrodynamic diameter distribution at 64 mM SDS with and without 10 000 ppm P123. All samples contained 0.1 mM NaCl.

SDS concentration that gave that ratio for 10 000 ppm P123 concentration.

Figure 5a shows that the total molar mass of the complexes decreased with increasing SDS concentration. For 10 000 ppm P123 with 1.25 mM SDS, the molar mass had decreased by ~85% relative to the SDS-free P123 micelles. This confirmed the progressive disintegration of the polymer micelles proposed by previous studies,[44,45] whereby the P123 micelles disintegrate into mixed micelles that contain fewer P123 chains per micelle as the SDS concentration is increased. Consistent with the accumulation of DS^- in the complexes and the corresponding electrostatic repulsions between complexes that would result, the second virial coefficient was positive and increased approximately 30-fold as the SDS concentration was increased to 1.25 mM in the presence of 10 000 ppm P123 (Figure 5b). The electrostatic repulsions between the complexes strengthened with increasing extents of SDS binding.

With a value for the molar mass of the complexes, the concentration of the complexes was simply calculated from the total SDS and P123 mass concentration involved in binding. The total SDS mass involved in binding was obtained by subtracting the mass of unbound free SDS and the mass of dissociated sodium ions among the bound SDS, assuming 23% counterion dissociation, from the mass of total added SDS. The mass of P123 involved in binding was the same as the mass of P123 added. The disintegration of the P123 micelles into less massive complexes increased the concentration of the P123/SDS mixed micelles that act as depletants. Increasing the total SDS concentration from 0 to 1.25 mM increased the P123/SDS mixed micelle molar concentration by a factor of 6.5 in the 10 000 ppm P123 solutions (Figure 5c).

Further insight into the relative amounts of SDS and P123 in the complexes can be gained by combining the binding isotherm results from the surfactant-selective electrode analysis (Figure 3) with the molar masses calculated from the Zimm analysis (Figure 5a). The numbers of SDS molecules N_{SDS} and of P123 molecules N_{P123} per P123/SDS complex were calculated as

$$N_{SDS} = \frac{C_{SDS}^{bound}}{C_{complex}}$$

and

$$N_{P123} = \frac{M_{com} - M_{DS}N_{SDS} - (1 - 0.23)M_{Na}N_{SDS}}{M_{P123}}$$

where C_{SDS}^{bound} is the total molar concentration of DS^- bound to the complexes, $C_{complex}$ is the total molar concentration of the complexes, M_{com} is the molar mass of the complexes, M_{DS} is the molar mass of DS^- ions, M_{P123} is the molar mass of P123, and M_{Na} is the molar mass of Na^+ ions. It is important to note here that the total number of SDS molecules bound, N_{SDS}, represents the total number of dodecyl sulfate ions bound, out of which 23% do not have sodium ions associated with them. These surfactant and polymer numbers are plotted in Figure 5d.

In the absence of SDS, the P123 aggregation number was ~75. This value is consistent with reported P123 micelle aggregation numbers of ~81−86 that were determined by small-angle neutron and X-ray scattering techniques.[68] When SDS is introduced, the SDS-free P123 micelles with 75 polymer chains per micelle first disintegrate into P123-rich mixed micelles at low SDS concentrations and then further disintegrate into mixed micelles with approximately equal numbers of P123 and SDS molecules per micelle, i.e., 11 and 8, respectively, at 1.25 mM SDS. Larger SDS concentrations were not considered in the static light scattering analysis due to the formation of bimodal distributions revealed by dynamic light scattering for those conditions. The evidence for the formation of the SDS-rich mixed micelles at high SDS concentrations is reported in Figure 3, where surfactant-selective electrode data indicated an average of 70 SDS per P123 in the complexes at the highest SDS concentration considered, 131 mM.

These static light scattering results indicate that the disintegration of the uncharged P123 micelles into a higher concentration of less massive but charged mixed micelles, at SDS concentrations as low as ~0.1 mM, is a significant contributor to the depletion force synergism that first occurred at 2 mM SDS concentrations. Increasing depletant charge and concentration both favor stronger depletion attraction. The dynamic light scattering results below support that mechanism and also give insight into the weakening and disappearance of depletion force synergism at the higher SDS concentrations.

Dynamic Light Scattering. Since the depletion interaction is sensitive to the size of the depletant, and static light scattering did not yield radius of gyration information, dynamic light scattering was used to determine the hydrodynamic diameters of the species present in solution for varying SDS

https://dx.doi.org/10.1021/acs.langmuir.0c01574
Langmuir 2020, 36, 10772−10784

concentrations with a fixed P123 concentration of 10 000 ppm. The hydrodynamic diameter distributions exhibited significant qualitative changes with increasing SDS concentration (Figure 6). Since these distributions were obtained from the distribution of diffusion coefficients, and diffusion coefficients for highly charged species are more sensitive to concentration than are nonionic species, the diffusion coefficient distributions were checked at three different P123 concentrations, 50 000, 20 000, and 10 000 ppm, at a fixed SDS/P123 mass ratio of 0.006. The diffusion coefficients obtained were the same for the different P123 concentrations, $0.54 \pm 0.027 \times 10^{-10}$ m^2/s, so the distributions in Figure 6 were deemed to be valid representations of the size distributions.

Surfactant-free P123 micelles were 18 nm in hydrodynamic diameter with a monomodal distribution, consistent with prior dynamic light scattering reports.[44] Addition of 1 mM SDS maintained a monomodal distribution and decreased the hydrodynamic diameter to 5 nm. This decrease in size was consistent with the static light scattering result that the molar mass of the complexes decreased by ∼85% upon addition of 1.25 mM SDS, and it further supported the progressive P123 micelle disintegration pathway. The monomodal size distribution was also consistent with the well-behaved Zimm plots that showed only a single type of scatterers existed up to 1.25 mM SDS. The decreased depletant size in the presence of 1.25 mM SDS would tend to decrease the magnitude and range of depletion forces.[69] The observation (Figure 1) that 2 mM SDS synergistically enhanced the depletion attraction shows that the increases in the depletant concentration (Figure 5) and the depletant charge (Figures 3 and 5) more than compensated for the size decrease at lower SDS concentrations in terms of the strength of the depletion attraction.

Further increasing the SDS concentration beyond 1 mM yielded a bimodal size distribution. For 2 and 4 mM SDS solutions, the larger diameter peak was similar to the hydrodynamic diameter of the SDS-free P123 micelles, and it dominated the intensity-weighted distribution. There was a minor contribution from a peak near 2 nm. This was likely due to coexistence of larger P123-rich mixed micelles and smaller SDS-rich mixed micelles. Increasing the SDS concentration to 32 mM maintained the bimodal distribution but now with the smaller diameter peak dominating the distribution. This would most likely result from the increasing prevalence of the SDS-rich mixed micelles at the higher SDS concentrations. The coexistence of two distinct types of depletants with different size and charge under these conditions was correlated with the appearance of a secondary attractive minimum in the force profile, which was unusual in the sense that the primary and secondary minima were not separated by a well-formed repulsive barrier (Figure 1b). The two force minima were separated by a local maximum that was in fact a weak attraction. This was discussed above in the context of the force measurements. Here, the dynamic light scattering results support the argument that this behavior resulted from distinct contributions from two different types of depletants acting at different separation distances.

Finally, at 64 mM SDS, the size distribution was again monomodal and indistinguishable from the size distribution of the polymer-free SDS micelles (Figure 6b). At the highest SDS concentration where colloidal forces were measured, all depletants were SDS-rich mixed micelles that were nearly indistinguishable from SDS micelles in terms of size (Figure 6b) and surfactant aggregation number and therefore charge (Figure 3). As a result, the depletion forces were barely distinguishable between the P123/SDS mixtures and the polymer-free SDS solutions at 64 mM SDS. Depletion force synergism was lost because the SDS-rich mixed micelles behaved as the SDS micelles would.

CONCLUSIONS

Colloidal probe atomic force microscopy measurements showed that mixed solutions of nonionic Pluronic P123 and anionic sodium dodecyl sulfate surfactants exhibit synergistic enhancement of depletion forces within a finite SDS concentration range that commences well below the normal CMC of SDS. In that regard, the P123/SDS system qualitatively resembles the previously examined Pluronic F108/SDS system.[17] However, the qualitative similarity of the trends in depletion forces belie significant differences in the underlying mixed self-assembly behaviors that produce the depletion forces in these two systems. In the current study, the P123 concentration was far above its CMC, whereas the F108 system was far below its CMC in the previous study. The combination of dodecyl sulfate-selective electrode analysis, static light scattering, and dynamic light scattering showed that the P123/SDS system was far richer in its self-assembly behavior.

SDS binding to unimeric F108 increased the size of the complexes until reaching a maximum, while increasing the charge all at a constant concentration of depletants. Those size trends are the opposite of those determined here for the P123/SDS system. The current study confirmed the previously proposed progression of complexation via micelle disintegration,[44,45] whereby SDS binding disintegrates the P123 micelles into more abundant mixed micelles that contain fewer polymer chains. With increasing extents of SDS/P123 complexation, the depletants increased in charge and concentration. That increase in depletant concentration is a primary cause of the depletion force synergism in the P123/SDS system. At high SDS concentrations, each of the characterization tools deployed here showed that the system evolved toward a state dominated by the SDS-rich mixed micelles that closely resembled the polymer-free SDS micelles. Accordingly, depletion force synergism disappeared at high SDS concentrations.

The current system, where the polymers and surfactants are mutually attractive, also displayed some similarities to depletion forces in the presence of the mutually repellant anionic SDS surfactants and sodium poly(acrylate) polyelectrolytes (PAA). At intermediate SDS concentrations in the P123/SDS system, secondary attractive force minima were separated not by a repulsive barrier as is normally observed for oscillatory structural forces with monodisperse depletants,[17,20,31,32] but by a local force maximum that was indeed weakly attractive. Similar behavior in the SDS/PAA system was attributed to redistribution of distinct depletants at different distance scales. This force behavior occurred in the P123/SDS system under conditions where dynamic light scattering confirmed the presence of two distinct types of complexes in solution that could also act at different separation distances, just as the SDS micelles and PAA chains did.

In a general sense, this work enhances the fundamental understanding of colloidal forces in the multicomponent systems containing two types of micelle-forming species that self-assemble into mixed micellar complexes. Such systems are common in formulated complex fluid products, and the current

https://dx.doi.org/10.1021/acs.langmuir.0c01574
Langmuir 2020, 36, 10772−10784

study establishes important possibilities for how colloidal interaction forces can respond to changing solution compositions. The intensity of synergistic colloidal force effects should be considered while formulating multicomponent complex fluid products. Because of these synergistic effects, colloidal forces that operate in multicomponent systems, and the macroscopic behaviors they generate, cannot be predicted from their isolated single-component studies.

■ ASSOCIATED CONTENT

Supporting Information

The Supporting Information is available free of charge at https://pubs.acs.org/doi/10.1021/acs.langmuir.0c01574.

Dodecyl sulfate ion-selective electrode construction; schematic of the potentiometric measurement with dodecyl sulfate ion-selective electrode; representative normalized force profiles for various SDS concentrations with 10 000 ppm P123 at 22 ± 2 °C (PDF)

■ AUTHOR INFORMATION

Corresponding Author

Robert D. Tilton − *Department of Chemical Engineering, Center for Complex Fluids Engineering and Department of Biomedical Engineering, Center for Complex Fluids Engineering, Carnegie Mellon University, Pittsburgh, Pennsylvania 15213, United States;* orcid.org/0000-0002-6535-9415; Phone: 1-412-268-1159; Email: tilton@cmu.edu

Author

Bhagyashree J. Lele − *Department of Chemical Engineering, Center for Complex Fluids Engineering, Carnegie Mellon University, Pittsburgh, Pennsylvania 15213, United States;* orcid.org/0000-0002-0677-4504

Complete contact information is available at: https://pubs.acs.org/10.1021/acs.langmuir.0c01574

Notes

The authors declare no competing financial interest.

■ ACKNOWLEDGMENTS

This material is based on work supported by the National Science Foundation under Grant CBET-1608003. The authors thank the PPG Industries Colloids, Polymers and Surfaces Lab at Carnegie Mellon University for access to light scattering and refractometry instruments.

■ REFERENCES

(1) Israelachvili, J. *Intermolecular and Surface Forces*; Elsevier, 2011.
(2) Liang, W.; Tadros, T. F.; Luckham, P. F. Flocculation of Sterically Stabilized Polystyrene Latex Particles by Adsorbing and Nonadsorbing Poly(acrylic Acid). *Langmuir* **1994**, *10*, 441−446.
(3) Napper, D. Steric Stabilization. *J. Colloid Interface Sci.* **1977**, *58*, 390−407.
(4) Lu, C.; Pelton, R. PEO Flocculation of Polystyrene-Core Poly(vinylphenol)-Shell Latex: An Example of Ideal Bridging. *Langmuir* **2001**, *17*, 7770−7776.
(5) Biggs, S.; Dagastine, R. R.; Prieve, D. C. Oscillatory Packing and Depletion of Polyelectrolyte Molecules at an Oxide-Water Interface. *J. Phys. Chem. B* **2002**, *106*, 11557−11564.
(6) Théodoly, O.; Tan, J. S.; Ober, R.; Williams, C. E.; Bergeron, V. Oscillatory Forces from Polyelectrolyte Solutions Confined in Thin Liquid Films. *Langmuir* **2001**, *17*, 4910−4918.
(7) Fielden, M. L.; Hayes, R. A.; Ralston, J. Oscillatory and Ion-Correlation Forces Observed in Direct Force Measurements between Silica Surfaces in Concentrated CaCl2 Solutions. *Phys. Chem. Chem. Phys.* **2000**, *2*, 2623−2628.
(8) Christov, N. C.; Danov, K. D.; Zeng, Y.; Kralchevsky, P. A.; Von Klitzing, R. Oscillatory Structural Forces due to Nonionic Surfactant Micelles: Data by Colloidal-Probe AFM vs Theory. *Langmuir* **2010**, *26*, 915−923.
(9) Asakura, S.; Oosawa, F. Interaction between Particles Suspended in Solutions of Macromolecules. *J. Polym. Sci.* **1958**, *33*, 183−192.
(10) Asakura, S.; Oosawa, F. On Interaction between Two Bodies Immersed in a Solution of Macromolecules. *J. Chem. Phys.* **1954**, *22*, 1255−1256.
(11) Milling, A. J.; Vincent, B. Depletion Forces between Silica Surfaces in Solutions of Poly(acrylic Acid). *J. Chem. Soc., Faraday Trans.* **1997**, *93*, 3179−3183.
(12) Piech, M.; Walz, J. Y. Depletion Interactions Produced by Nonadsorbing Charged and Uncharged Spheroids. *J. Colloid Interface Sci.* **2000**, *232*, 86−101.
(13) Kralchevsky, P. A.; Danov, K. D.; Anachkov, S. E. Depletion Forces in Thin Liquid Films due to Nonionic and Ionic Surfactant Micelles. *Curr. Opin. Colloid Interface Sci.* **2015**, *20*, 11−18.
(14) Walz, J. Y.; Sharma, A. Effect of Long Range Interactions on the Depletion Force between Colloidal Particles. *J. Colloid Interface Sci.* **1994**, *168*, 485−496.
(15) Ji, S.; Walz, J. Y. Interaction Potentials between Two Colloidal Particles Surrounded by an Extremely Bidisperse Particle Suspension. *J. Colloid Interface Sci.* **2013**, *394*, 611−618.
(16) Lele, B. J.; Tilton, R. D. Colloidal Depletion and Structural Force Synergism or Antagonism in Solutions of Mutually Repelling Polyelectrolytes and Ionic Surfactants. *Langmuir* **2019**, *35*, 15937−15947.
(17) Lele, B. J.; Tilton, R. D. Control of the Colloidal Depletion Force in Nonionic Polymer Solutions by Complexation with Anionic Surfactants. *J. Colloid Interface Sci.* **2019**, *553*, 436−450.
(18) Pagac, E. S.; Tilton, R. D.; Prieve, D. C. Depletion Attraction Caused by Unadsorbed Polyelectrolytes. *Langmuir* **1998**, *14*, 5106−5112.
(19) Odiachi, P. C.; Prieve, D. C. Effect of Added Salt on the Depletion Attraction Caused by Non-Adsorbing Clay Particles. *Colloids Surf., A* **1999**, *146*, 315−328.
(20) Biggs, S.; Prieve, D. C.; Dagastine, R. R. Direct Comparison of Atomic Force Microscopic and Total Internal Reflection Microscopic Measurements in the Presence of Nonadsorbing Polyelectrolytes. *Langmuir* **2005**, *21*, 5421−5428.
(21) Herman, D.; Walz, J. Y. Adsorption and Stabilizing Effects of Highly-Charged Latex Nanoparticles in Dispersions of Weakly-Charged Silica Colloids. *J. Colloid Interface Sci.* **2015**, *449*, 143−151.
(22) McKee, C. T.; Walz, J. Y. Interaction Forces between Colloidal Particles in a Solution of like-Charged, Adsorbing Nanoparticles. *J. Colloid Interface Sci.* **2012**, *365*, 72−80.
(23) Piech, M.; Walz, J. Y. Analytical Expressions for Calculating the Depletion Interaction Produced by Charged Spheres and Spheroids. *Langmuir* **2000**, *16*, 7895−7899.
(24) Rudhardt, D.; Bechinger, C.; Leiderer, P. Direct Measurement of Depletion Potentials in Mixtures of Colloids and Nonionic Polymers. *Phys. Rev. Lett.* **1998**, *81*, 1330−1333.
(25) Ruths, M.; Yoshizawa, H.; Fetters, L. J.; Israelachvili, J. N. Depletion Attraction versus Steric Repulsion in a System of Weakly Adsorbing Polymer-Effects of Concentration and Adsorption Conditions. *Macromolecules* **1996**, *29*, 7193−7203.
(26) Kuhl, T. L.; Berman, A. D.; Hui, S. W.; Israelachvil, J. N. Part 2. Crossover from Depletion Attraction to Adsorption: Polyethylene Glycol Induced Electrostatic Repulsion between Lipid Bilayers. *Macromolecules* **1998**, *31*, 8258−8263.
(27) Kuhl, T. L.; Berman, A. D.; Hui, S. W.; Israelachvili, J. N. Part 1. Direct Measurement of Depletion Attraction and Thin Film Viscosity between Lipid Bilayers in Aqueous Polyethylene Glycol Solutions. *Macromolecules* **1998**, *31*, 8250−8257.

(28) Sharma, A.; Tan, S. N.; Walz, J. Y. Effect of Nonadsorbing Polyelectrolytes on Colloidal Interactions in Aqueous Mixtures. *J. Colloid Interface Sci.* **1997**, *191*, 236−246.
(29) James, G. K.; Walz, J. Y. Experimental and Theoretical Investigation of the Depletion and Structural Forces Produced by Ionic Micelles. *Colloids Surf., A* **2014**, *441*, 406−419.
(30) James, G. K.; Walz, J. Y. Experimental Investigation of the Effects of Ionic Micelles on Colloidal Stability. *J. Colloid Interface Sci.* **2014**, *418*, 283−291.
(31) Tulpar, A.; Tilton, R. D.; Walz, J. Y. Synergistic Effects of Polymers and Surfactants on Depletion Forces. *Langmuir* **2007**, *23*, 4351−4357.
(32) Ji, S.; Walz, J. Y. Synergistic Effects of Nanoparticles and Polymers on Depletion and Structural Interactions. *Langmuir* **2013**, *29*, 15159−15167.
(33) Ji, S.; Walz, J. Y. Depletion Forces and Flocculation with Surfactants, Polymers and Particles - Synergistic Effects. *Curr. Opin. Colloid Interface Sci.* **2015**, *20*, 39−45.
(34) Goddard, E. D. *Interactions of Surfactants with Polymers and Proteins*; Goddard, E. D.; Ananthapadmanabhan, K. P., Eds.; CRC Press, 2018; Vol. *15*.
(35) Goddard, E. D. Polymer/Surfactant Interaction: Interfacial Aspects. *J. Colloid Interface Sci.* **2002**, *256*, 228−235.
(36) Guzmán, E.; Llamas, S.; Maestro, A.; Fernández-Peña, L.; Akanno, A.; Miller, R.; Ortega, F.; Rubio, R. G. Polymer-Surfactant Systems in Bulk and at Fluid Interfaces. *Adv. Colloid Interface Sci.* **2016**, *233*, 38−64.
(37) Tilton, R. D. Adsorption from Mixtures of Polymers and Surfactants, in *Encyclopedia of Surface and Colloid Science*, 2nd ed.; Taylor & Francis: New York, 2006; *1*, pp 256−270.
(38) Nambam, J. S.; Philip, J. Effects of Interaction of Ionic and Nonionic Surfactants on Self-Assembly of PEO-PPO-PEO Triblock Copolymer in Aqueous Solution. *J. Phys. Chem. B* **2012**, *116*, 1499−1507.
(39) Thurn, T.; Couderc, S.; Sidhu, J.; Bloor, D. M.; Penfold, J.; Holzwarth, J. F.; Wyn-Jones, E. Study of Mixed Micelles and Interaction Parameters for ABA Triblock Copolymers of the Type EOm-POn-EOm and Ionic Surfactants: Equilibrium and Structure. *Langmuir* **2002**, *18*, 9267−9275.
(40) Tam, K. C.; Wyn-Jones, E. Insights on Polymer Surfactant Complex Structures during the Binding of Surfactants to Polymers as Measured by Equilibrium and Structural Techniques. *Chem. Soc. Rev.* **2006**, *35*, 693.
(41) Li, Y.; Xu, R.; Couderc, S.; Bloor, M.; Wyn-Jones, E.; Holzwarth, J. F. Binding of Sodium Dodecyl Sulfate (SDS) to the ABA Block Copolymer Pluronic F127 (EO 97 PO 69 EO 97): F127 Aggregation Induced by SDS. *Langmuir* **2001**, *17*, 183−188.
(42) Mi, X.; Yuan, J.; Han, Y.; Liu, H.; Liu, H.; Gao, X.; Xu, C.; Zhang, J. Introduction of Anionic Surfactants to Copolymer Micelles: A Key to Improving Utilization Efficiency of P123 in Synthesis of Mesoporous Aluminosilicates. *Ind. Eng. Chem. Res.* **2017**, *56*, 7224−7228.
(43) Chaibundit, C.; Ricardo, N. M. P. S.; Costa, F. d. M. L. L.; Yeates, S. G.; Booth, C. Micellization and Gelation of Mixed Copolymers P123 and F127 in Aqueous Solution. *Langmuir* **2007**, *23*, 9229−9236.
(44) Jansson, J.; Schillén, K.; Olofsson, G.; Cardoso da Silva, R.; Loh, W. The Interaction between PEO-PPO-PEO Triblock Copolymers and Ionic Surfactants in Aqueous Solution Studied Using Light Scattering and Calorimetry. *J. Phys. Chem. B* **2004**, *108*, 82−92.
(45) da Silva, R. C.; Olofsson, G.; Schillén, K.; Loh, W. Influence of Ionic Surfactants on the Aggregation of Poly(ethylene Oxide)-Poly(propylene Oxide)-Poly(ethylene Oxide) Block Copolymers Studied by Differential Scanning and Isothermal Titration Calorimetry. *J. Phys. Chem. B* **2002**, *106*, 1239−1246.
(46) Bharatiya, B.; Ghosh, G.; Bahadur, P.; Mata, J. The Effects of Salts and Ionic Surfactants on the Micellar Structure of Tri-Block Copolymer PEO-PPO-PEO in Aqueous Solution. *J. Dispersion Sci. Technol.* **2008**, *29*, 696−701.
(47) Li, Y.; Xu, R.; Couderc, S.; Bloor, M.; Wyn-Jones, E.; Holzwarth, J. F. Binding of Sodium Dodecyl Sulfate (SDS) to the ABA Block Copolymer Pluronic F127 (EO 97 PO 69 EO 97): F127 Aggregation Induced by SDS. *Langmuir* **2001**, *17*, 183−188.
(48) Ganguly, R.; Aswal, V. K.; Hassan, P. A.; Gopalakrishnan, I. K.; Kulshreshtha, S. K. Effect of SDS on the Self-Assembly Behavior of the PEO−PPO−PEO Triblock Copolymer (EO) 20 (PO) 70 (EO) 20. *J. Phys. Chem. B* **2006**, *110*, 9843−9849.
(49) Ducker, W.; Senden, T. J.; Pashley, R. M. Direct Measurement of Colloidal Forces Using an Atomic Force Microscope. *Nature* **1991**, *353*, 239−241.
(50) Green, C. P.; Lioe, H.; Cleveland, J. P.; Proksch, R.; Mulvaney, P.; Sader, J. E. Normal and Torsional Spring Constants of Atomic Force Microscope Cantilevers. *Rev. Sci. Instrum.* **2004**, *75*, 1988−1996.
(51) Tulpar, A.; Walz, J. Y. Simultaneous Measurement of Structural and Hydrodynamic Forces between Colloidal Surfaces in Complex Fluids. *Colloids Surf., A* **2007**, *300*, 268−280.
(52) Beaglehole, D. Ellipsometric Study of the Surface of Simple Liquids. *Phys. B + C* **1980**, *100*, 163−174.
(53) Saigal, T.; Riley, J. K.; Golas, P. L.; Bodvik, R.; Claesson, P. M.; Matyjaszewski, K.; Tilton, R. D. Poly(ethylene Oxide) Star Polymer Adsorption at the Silica/aqueous Interface and Displacement by Linear Poly(ethylene Oxide). *Langmuir* **2013**, *29*, 3999−4007.
(54) Riley, J. K.; Matyjaszewski, K.; Tilton, R. D. Electrostatically Controlled Swelling and Adsorption of Polyelectrolyte Brush-Grafted Nanoparticles to the Solid/liquid Interface. *Langmuir* **2014**, *30*, 4056−4065.
(55) De Feijter, J. A.; Benjamins, J.; Veer, F. A. Ellipsometry as a Tool to Study the Adsorption Behavior of Synthetic and Biopolymers at the Air−water Interface. *Biopolymers* **1978**, *17*, 1759−1772.
(56) Huang, Y.-R.; Lamson, M.; Matyjaszewski, K.; Tilton, R. D. Enhanced Interfacial Activity of Multi-Arm Poly(ethylene Oxide) Star Polymers Relative to Linear Poly(ethylene Oxide) at Fluid Interfaces. *Phys. Chem. Chem. Phys.* **2017**, *19*, 23854−23868.
(57) Braem, A. D.; Prieve, D. C.; Tilton, R. D. Electrostatically Tunable Coadsorption of Sodium Dodecyl Sulfate and Poly(ethylene Oxide)-B-Poly(propylene Oxide)-B-Poly(ethylene Oxide) Triblock Copolymer to Silica. *Langmuir* **2001**, *17*, 883−890.
(58) Wang, J.; Du, Z.; Wang, W.; Xue, W. Ion-Selective Electrode for Anionic Surfactants Using Hexadecyl Trimethyl Ammonium Bromide-Sodium Dodecylsulfate as an Active Ionophore. *Int. J. Electrochem.* **2011**, *2011*, No. 958647.
(59) Bandyopadhyay, A.; Moulik, S. P. Counterion Binding Behaviour of Micelles of Sodium Dodecyl Sulphate and Bile Salts in the Pure State, in Mutually Mixed States and Mixed with a Nonionic Surfactant. *Colloid Polym. Sci.* **1988**, *266*, 455−461.
(60) Mikhelson, K. N. *Ion-Selective Electrodes; Lecture Notes in Chemistry*; Springer: Berlin, 2013; Vol. *81*.
(61) Alexandridis, P.; Holzwarth, J. F.; Hatton, T. A. Micellization of Poly(ethylene Oxide)-Poly(propylene Oxide)-Poly(ethylene Oxide) Triblock Copolymers in Aqueous Solutions: Thermodynamics of Copolymer Association. *Macromolecules* **1994**, *27*, 2414−2425.
(62) Prausnitz, J. M.; Lichtenthaler, R. N.; de Azevedo, E. G. *Molecular Thermodynamics of Fluid-Phase Equilibria*, 3rd ed.; Prentice-Hall: Upper Saddle River, NJ, 1999.
(63) Pashley, R. M.; Ninham, B. Double-Layer Forces in Ionic Micellar Sotutions. *J. Phys. Chem. A.* **1987**, *91*, 2902−2904.
(64) Nishikido, N. Estimation of Micellar Charge or Aggregation Number from Conductivity and Counterion-Activity Measurements. *J. Colloid Interface Sci.* **1983**, *92*, 588−591.
(65) Evans, H. C. 117. Alkyl Sulphates. Part I. Critical Micelle Concentrations of the Sodium Salts. *J. Chem. Soc.* **1956**, No. 579.
(66) Brown, W.; Fundin, J.; Miguel, M. d. G. Poly(ethylene Oxide)-Sodium Dodecyl Sulfate Interactions Studied Using Static and Dynamic Light Scattering. *Macromolecules* **1992**, *25*, 7192−7198.

https://dx.doi.org/10.1021/acs.langmuir.0c01574
Langmuir 2020, 36, 10772−10784

(67) Bodycomb, J.; Hara, M. Light Scattering Study of Ionomers in Solution. 4. Angular Measurements of Sulfonated Polystyrene Ionomers in a Polar Solvent (Dimethylformamide). *Macromolecules* **1994**, *27*, 7369−7377.
(68) Manet, S.; Lecchi, A.; Impe′ror-Clerc, M.; Zholobenko, V.; Durand, D.; Oliveira, C. L. P.; Pedersen, J. S.; Grillo, I.; Meneau, F.; Rochas, C. Structure of Micelles of a Nonionic Block Copolymer Determined by SANS and SAXS. *J. Phys. Chem. B* **2011**, *115*, 11318−11329.
(69) Ji, S.; Walz, J. Y. Depletion Flocculation Induced by Synergistic Effects of Nanoparticles and Polymers. *J. Phys. Chem. B* **2013**, *117*, 16602−16609.

https://dx.doi.org/10.1021/acs.langmuir.0c01574
Langmuir 2020, 36, 10772−10784